Arch. Metall. Mater. **62** (2017), 1, 407-413

DOI: 10.1515/amm-2017-0062

L. KUCHARIKOVÁ*#, E. TILLOVÁ*, M. MATVIJA**, J. BELAN*, M. CHALUPOVÁ*

STUDY OF THE PRECIPITATION HARDENING PROCESS IN RECYCLED Al-Si-Cu CAST ALLOYS

The formation of extremely small uniformly dispersed particles of a second phase within the original phase matrix during heat treatment changed material properties. Therefore the characterization of precipitation had been investigated using high resolution transmission electron microscopy (TEM) and electron diffraction of thin foils for an AlSi9Cu3 cast alloy. For investigation the hardening effect onto mechanical properties of aluminium cast was used heat treatment, which consisted from solution treatment at 515°C / 4 hours (h), followed by quenching into water with temperature 50°C and artificial aging using different temperatures 170°C and 190°C with different holding time 2, 4, 8, 16, and 32 hours. The observations of microstructure and substructure reveals that precipitation hardening has caused great changes in size, morphology and distributions of structural components, the formation of precipitates of Cu phases, and the change of mechanical properties as well.

Keywords: recycled Al-Si-Cu cast alloys, precipitation hardening, Cu precipitate, mechanical properties, and transmission electron microscopy

1. Introduction

Recycling is one of the possibilities how reuse the aluminium scrap, and at the same time thinking on economic and ecological implications. The previous works have shown that production of 1 kg secondary Al alloys by recycling requires about 2.8 kWh, while production of 1 kg primary Al alloys requires about 45 kWh. Also producing aluminium by recycling creates only about 4% as much CO_2 as by primary production [1]. These facts are important conclusions for the aluminium industry throughout the world because growing usage of aluminium alloys in different application mostly in aerospace and automotive industry cause increase demand for these materials. The most common aluminium alloy used in aerospace and automotive industry is aluminium material group Al-Si. This type of material comprising 85% to 90% of the aluminium cast parts produced for the automotive industry. It is probably thanks its positive properties such as excellent castability, good corrosion and wear resistance, high strength stiffness to weight ratio, low density and thermal expansion, high productivity and low shrinkage rate, recycling possibilities, and low cost, also can be given a wide variety of surface finishes and it can be cast and produced into almost any form of product. It is not surprisingly that aluminium has become prime importance as engineering material with all these outstanding properties [2-9]. Therefore it is necessary to study interaction of microstructure and properties. Properties of Al-Si cast alloys are more influenced by morphology, shape and distribution of matrix, Si particles, second phases and defects. These structural features are influenced with the composition, melt treatment conditions, grain refining, modification, solidification rate, casting process, heat treatment, and so on [10-13]. Producers of aluminium casts increase the tensile strength and yield strengths with heat treating. Precipitation hardening heat treatment is the most commonly used process to obtain the optimal combination of strength and ductility of Al-Si-Cu casts. Precipitation hardening is a process that enhances the strength and hardness of metal alloys by the formation of extremely small uniformly dispersed particle of a second phase within the original phase matrix [4,14].

The precipitation hardening process involves three basic steps [15-19]:

- First step: solution treatment – the alloy is heated above the solvus temperature, maintaining this temperature in order to dissolution all Cu or Mg in the solid solution as a stable fcc α phase until a homogeneous solid solution (α) is produced. The θ precipitates are dissolved in this step and any segregation present in the original alloy is reduced.
- Second step: rapid quenching (cooling at critical or higher speed) – the solid α is rapidly quenchid and a supersaturated solid solution of α_{SS} which contains excess Cu or Mg is forming. It is not an equilibrium structure. The atoms do not have time to diffuse to potential nucleation sites and thus θ precipitates do not form.
- Third step: aging – the supersaturated α, α_{SS}, is heated below the solvus temperature to produce a finely dispersed precipitate. It can be realized at room temperature – natural ageing, or at the higher temperature – artificial aging.

* UNIVERSITY OF ŽILINA, FACULTY OF MECHANICAL ENGINEERING, UNIVERZITNÁ 8215/1, 010 26 ŽILINA, SLOVAKIA
** TECHNICAL UNIVERSITY OF KOŠICE, FACULTY OF METALLURGY, LETNÁ 9, 042 00 KOŠICE, SLOVAKIA

Corresponding author: Lenka.Kucharikova@fstroj.uniza.sk

Precipitation in commercial aluminium alloys usually starts from the formation of GP zones, which may be regarded as fully coherent metastable precipitates. Subsequent evolution of the microstructure involves the replacement of the GP zones with more stable phases. The sequence is described as $\alpha_{ss} \rightarrow$ GP zones $\rightarrow \theta' \rightarrow \theta$ (e.g. Al_2Cu). The typical size of GP zones is in the order of tens of nanometers. These particles or small solute-rich clusters are completely coherent with matrix, and are invisible in the optical microscope but macroscopically, this change is observed as an increase in the hardness and tensile strength of the alloy [20].

The proces of precipitation hardening in material Al-Si-Cu is complicated, because according to Belov [22] in this type of material can precipitate the phases of Si, Al_2Cu, Al_2CuMg (S-phase), Al_7Cu_2Fe, $Al_6(FeCu)$ (marked as $Al_{23}CuFe_4$), $Al_5Cu_2Mg_8Si_6$ (Q-phase), Mg_2Si, Al_8Fe_2Si, Al_5FeSi (β-phase), $Al_8FeMg_3Si_6$ (π-phase), Al_7Cu_2Fe (N-phase), $Al_{15}(FeMn)_3Si_2$, and at higher content of Mg – Al_8Mg_5 and Al_6CuMg_4 phases. These´s stable equilibrium phases preceding the phases which are nonequilibrium coherent and semi-coherent with the aluminum matrix. Therefore the main objective of this work was to study of precipitation hardening process in AlSi9Cu3 cast alloy. The present work is a part of large research project N° 01/0533/15, which was conducted to investigate and to provide a better understanding microstructure and properties of recycled Al-Si cast alloys.

2. Experimental

2.1. Experimental Material

The secondary (prepared by recycling of aluminium scrap) hypoeutectic AlSi9Cu3 alloy was used for experimental study. The alloy was received in the form of 12.5 kg ingots. Experimental material was molten and purified with salt AlCu4B6 before casting and was not modified or grain refined. Then molten material was gravity die cast into the metallic mould with cast bars dimensions Ø 15 × 180 mm. The chemical analysis of bars from recycled AlSi9Cu3 cast alloy was carried out using an arc spark spectroscopy at University of Žilina. The results are shown in Table 1.

AlSi9Cu3 cast alloy has lower corrosion resistance and is suitable for high temperature applications (dynamic exposed casts, where are not so big requirements on mechanical properties) – it means to max. 250°C. The primary AlSi9Cu3 alloy has these technological properties: ultimate tensile strength (UTS = 240-310 MPa), offset 0.2% yield stress (140-240 MPa), however the low elongation limits (A_5 = 0.5-3%) and hardness HB 80-120, density 2.65 kg.dm^{-3}, good castability and machinability, adequate polishability and bad weldability and corrosion resistance [23]. Thanks to its properties this alloy is used in the automotive industry for the production of cylinder heads, pistons, engine mounts, heat exchangers, air conditioners, transmissions housings, wheels, fenders etc. [24].

2.2. Experimental Methods

Testing specimens (for tensile test and bending impact test) were made from bars by turning and milling operations. The specimens were precipitation hardened before testing (solution treatment at 515°C / 4h, water quenching at 50°C and artificial aging at different temperature 170°C and 190°C with different holding time 2, 4, 8, 16 and 32 hours [11,25,26].

Mechanical properties were measured according to the following standards: STN EN ISO 6892-1, STN EN ISO 148-1 and STN EN ISO 6506-1. Hardness measurement for secondary aluminum alloy was performed by using Brinell hardness tester with load of 62.5 kp (1 kp = 9.80665 N), testing ball with 2.5 mm diameter and a dwell time of 15 s. Ultimate tensile strength was measured using ZDM 30 testing machine. The impact energy was measured with using of pendulum – Charpy´s hammer. The evaluated Brinell hardness, UTS, elongation and impact energy reflect average values of at least six separate bars on each temperature and holding time.

The samples for metallography observation were prepared from selected tensile specimens (after testing) and the microstructures were studied using an optical microscope Neophot 32 and a scanning electron microscope VEGA LMU II. Samples were prepared by standard metallographic procedures. Some samples were also deep-etched for 30 s in HCl solution in order to reveal the three-dimensional morphology of the silicon phase and intermetallic phases with using scanning electron microscopy.

The analysis of alloy substructure was realized using Jeol JEM-2000FX transmission electron microscope and identification of particles was performed using the selected area electron diffraction (SAED) inside TEM. The specimens for substructure analysis were taken from specimens for bending impact test after testing from areas that were not affected by deformation at bending impact test or during production specimens for mechanical test. Specimens were taken by Struers Secotom-10 to form of thin plates and then were mechanically thinned by grinding and polishing (to a thikness of ~100 μm). Subsequently, the samples were electrolytic polished by Struers TenuPol-5 in solution of 33 % nitrid acid and 67 % methanol, while the temperature was maintained at – 35°C and voltage at 16 V. Evaluation of average size (width, length, thicknes) of particles in alloy substructure and their number per unit area (amount) was carried out by standart statistical methods.

TABLE 1

Chemical analysis of the casting specimen made of the AlSi9Cu3, in wt. %

Si	Cu	Mn	Zn	Mg	Ni	Pb	Fe	Ti	Sn	Cr	Al
10.66	2.28	0.305	1.01	0.265	0.103	0.120	1.02	0.04	0.04	0.05	balance

3. Results and discussion

3.1. Mechanical properties

Mechanical properties of Al-Si alloys are largely dependent upon an appropriate heat treatment technology. During precipitation hardening – T6, series of changes in microstructure have occured (e.g. the dissolution of precipitates, the homogenization of the cast structure, such as the minimization of alloying element segregation, the spheroidization and coarsening of eutectic silicon and the precipitation of finer Al_2Cu or Mg_2Si hardening phase), which then leads to the improvement of mechanical properties. Because the morphology, the amount and the distribution of the precipitates during aging process significantly influence the mechanical properties, it is very important to investigate the effects of heat treatment on the alloys [11].

Influence of heat treatments onto mechanical properties (ultimate strength tensile – UTS; Brinell hardness – HBW; Elongation (A_5); and Impact energy (E)) for recycled AlSi9Cu3 cast alloy is shown on Fig. 1. The Fig. 1 shows mechanical properties after solution treatment (T4 = 515°C – blue curve) and after two different artificial aging temperatures (T6 = 515°C / 4 h + 170°C – orange curve or 515°C / 4 h + 190°C – grey curve) for comparising their effect, but also shows mechanical properties of secondary AlSi9Cu3 cast alloy in as-cast state which are: UTS = 211 MPa; 98 HBW 2.5 / 62.5 / 15; A_5 = 1.3 % and E = 3 J. These results and previous work shows that secondary (recycled) aluminium cast alloys have comparable properties as primary aluminium alloys [23]. The Brinell hardness results show that there is an obvious precipitation hardening phenomenon for each curve. The best precipitation hardening phenomenon is observed on curve at temperature 190°C of artificial aging (Fig. 1a). The heat treatment T4 shows only the first peak of aging and than intermediate stage of aging – the hardness decrease and do not increase again (Fig. 1a). For samples aged at temperature 170°C of artificial aging a single aging peak and next hardness high plateau was observed (Fig. 1a). The results (Fig. 1) show that solution heat treatment improved some of mechanical properties compared to the as-cast state of secondary AlSi9Cu3 alloy, but precipitation hardening has greater influence onto mechanical properties improvement. The highest hardness was measured on samples heat treated at 170°C artificial aging (139 HBW 2.5 / 62.5 / 15 with holding time from 8 to 32 h) (Fig. 1a). Highest UTS and A_5 were measured for 190°C of artificial aging, but comparable results have the temperature 170°C, too (Fig. 1b,c). When compare results in first aging peak 170°C / 4 h = 276 MPa and 190°C / 4 h = 287 MPa, in the second aging peak 170°C / 16 h = 311 MPa and 190°C / 16 h = 309 MPa (Fig. 1b) for company is maybe better to use artificial aging at 170°C (at lower temperatures have castings comparable strength) due to lowering economic costs. Impact energy is for both temperature of artificial aging comparable (Fig. 1d).

These results show that optimal properties have specimens after precipitation hardening at 515°C / 4 h + 170°C / 16 h. Mechanical properties also shows that it is very important what mechanical properties are required, because in some case it will be worth to use only solution treatment for improving properties.

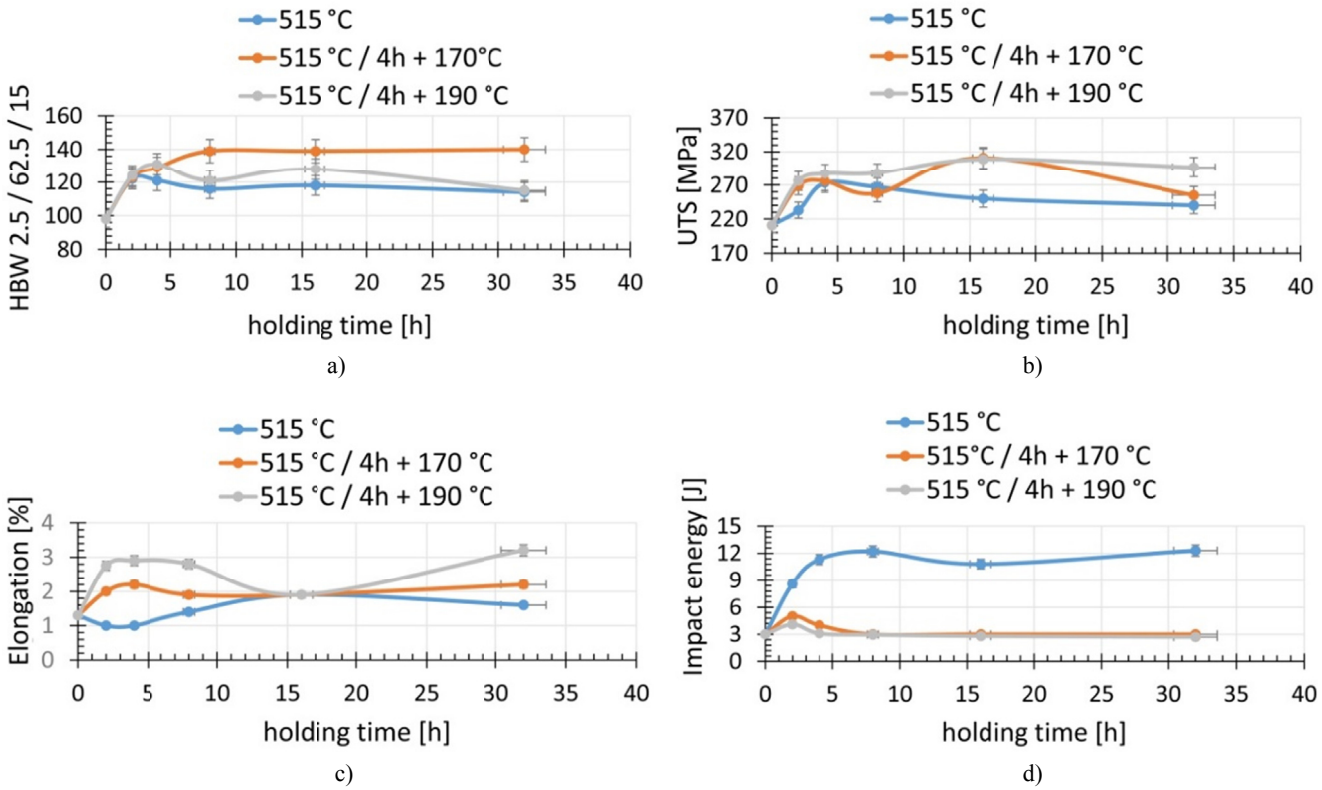

Fig. 1. Basic mechanical properties of secondary AlSi9Cu3 after treatment, a) Brinell hardness; b) Ultimate tensile strength; c) Elongation; d) Impact energy

3.2. Microstructure

However, optimum tensile, impact, and fatigue properties of aluminium alloys are obtained with small, spherical and evenly distributed particles it is neccesseary to study changes in microstructure too. Structure of hypoeutectic AlSi9Cu3 cast alloy consist of *α*-phase dendrites (light grey), eutectic (it is mechanical micture of α-phase and eutectic Si particles) and intermetallic phases of different chemical composition, mostly group Cu-rich and Fe-rich (Fig. 2a). In the microstructure of experimental material were observed first of all complex Fe-rich intermetallic phases $Al_{15}(Mn,Fe)_3Si_2$ (skeleton / script-like phase), a small amount of needle-like Al_5FeSi phase and Cu-rich phases primarily as Al-Al_2Cu-Si (called thernary eutectic)

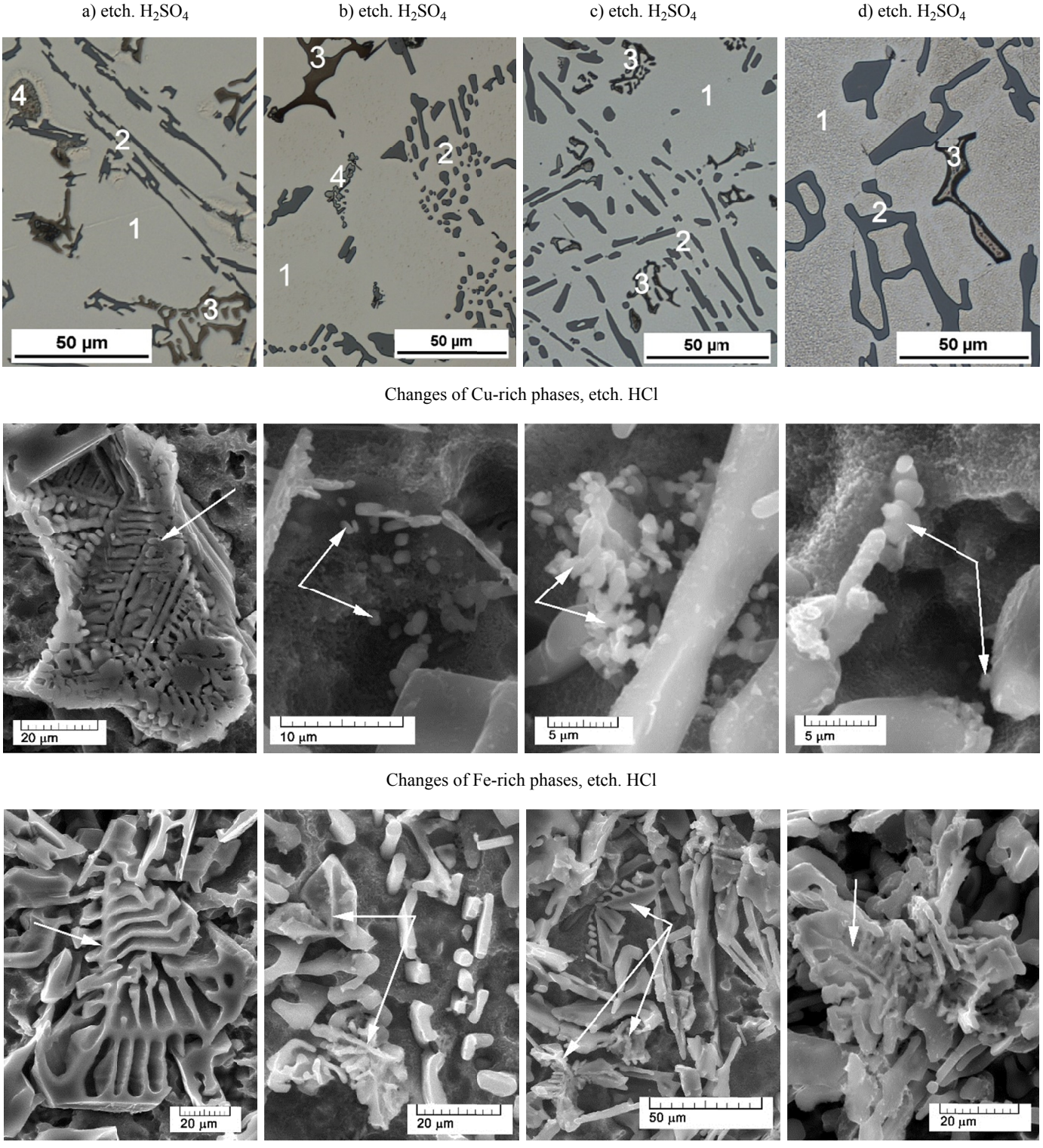

Fig. 2 Changes in microstructure after used heat treatment in secondary AlSi9Cu3 cast alloy. 1 – *α*-phase; 2 – eutectic; 3 – Fe-rich phases (especialy $Al_{15}(Mn,Fe)_3Si_2$); 4 – Cu-rich ternary eutectic. a) As-cast state; b) 515°C / 4h + room temperature / 24h; c) 515°C / 4h + 170°C / 16h; d) 515°C / 4h + 190°C / 16h.

but in some areas were observed Al_2Cu phases, too (Fig. 2a). Experimental material was not modified and that is why eutectic Si particles are in form of platelets (Fig. 2a – 2), which on metallographic cut are in form of needles (in as-cast state). The solution treatment is the most important parameter that influences the kinetics of Si morphology transformation during the course of solution treatment [10]. After solution treatment at the temperature of 515°C were noted that the Si platelets fragmented into smaller segments and these smaller Si particles were spheroidised into small rounded shape (Fig. 2b – 2). The precipitation hardening at temperature of artificial aging 170°C has caused fragmentation of long needles of Si particles which have spherical edges (Fig. 2c – 2). Higher temperature of artificial aging 190°C led to only small changes, because the eutectic Si particles were large (is observed Si coarsening) in comparison with the other experimental state (besides as-cast) (Fig. 2d – 2). Fe-rich phases are dissolved and fragmented to smaller particles. In as-cast samples phase $Al_{15}(MnFe)_3Si_2$ has a compact skeleton-like morphology (Fig. 2a – 3). Solution heat treatment does not make a greate changes in morphology of these particles (Fig. 2b – 3). The precipitation hardening (artificial aging 170°C) led to dissolution and fragmentation of compact phase to smaller skeleton particles (Fig. 2c – 3). The artificial aging 190°C led to fragmentation of Fe-rich phases, but these phases were still large (Fig. 2d – 3). Fe-needles were fragmented and dissolved, but vere only in small volume.

The ternary eutectic Al-Al_2Cu-Si without heat treatment (as-cast state) occurs in form of compact oval troops (Fig. 2a – 4). After solution treatment at temperature 515°C ternary eutectic disintegrated into the form of coarsened globular particles (Fig. 2b – 4) (some of them occurs along the needles, probably Fe-rich Al_5FeSi phase) and the amount of ternary eutectic decreases. The Al-Al_2Cu-Si is gradually dissolved into the surrounding Al-matrix with an increase in solution treatment time. The compact Al-Al_2Cu-Si disintegrates to separates Al_2Cu fibres after precipitation hardening.

3.3. Substructure

The previous work [25-26] shows that optimal solution heat treatment is at 515°C / 4 hours for specimens from these type of cast alloy. Cáceres [27] reported that metastabile θ'- Al_2Cu is the primary strengthening phase responsible for the precipitation hardening response produced by these alloys. Therefore a TEM was used for observation the precipitates formed during precipitation hardening, for which this method is the most effective. The substructure of as-cast alloy state is shown in (Fig. 3). In solid solution of alloy the needles particles or rod-shaped particles have been observed in the size range approx. 0.5 μm, as shown in (Fig. 3a). Using selected area electron diffraction they were identified as Si partiles crystallized in cubic system (Fig. 3b).

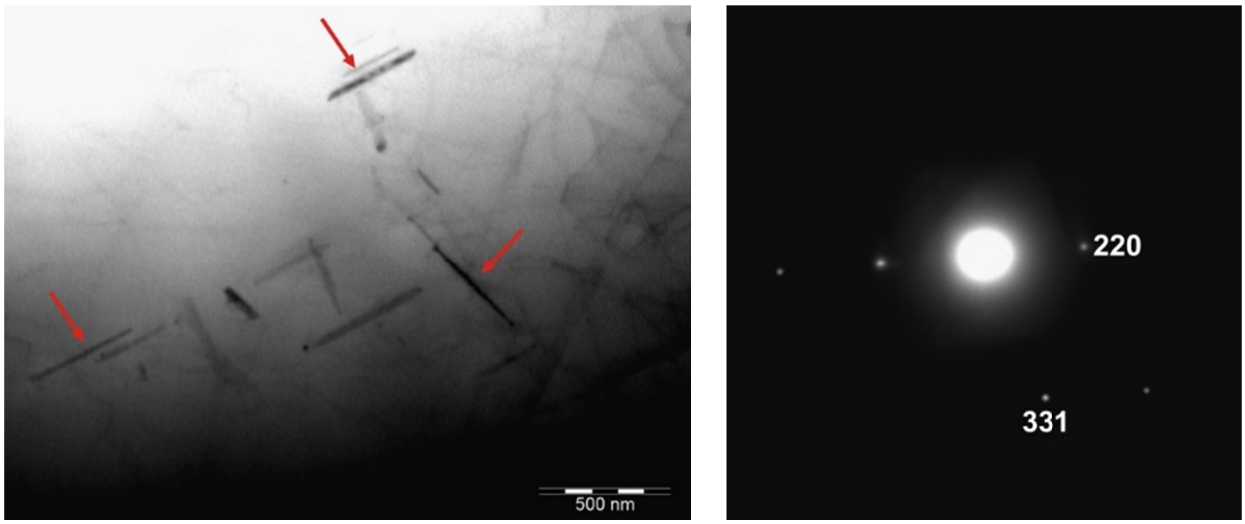

a) b)

Fig. 3 TEM micrographs of AlSi9Cu3 specimen in as-cast state; a) Si particles in solid solution (indicated by arrows); b) SAED of Si particle

However, the maximum hardness properties were identified on samples precipitation hardened at 170 C / 16 h of artificial aging, but UTS and A_5 were higher on specimens precipitation hardened at 190°C. The aim was to compare the substructure differences, which caused these changes (Fig. 4). The results show that after 16 hours three types of particles – oval, platelets and needles are observed in substructure of both specimens (Figs. 4a,b). All of these particles were identified as Al_2Cu phases = precipitates of tetragonal crystallography system using SAED into TEM (Fig. 4c). The differences were in their dimensions (Table 2). The (Table 2) shows measured values of precipitates of different morphology at two tempereatures of artificial aging.

From comparison of two alloy states it is clear that during artificial ageing of alloy at temperature 190°C, the amount of precipitates was significantly higher as a result of less nucleation barriers, while the average dimension did not change significantly. This fact was reflected in the development of the alloy mechanical properties.

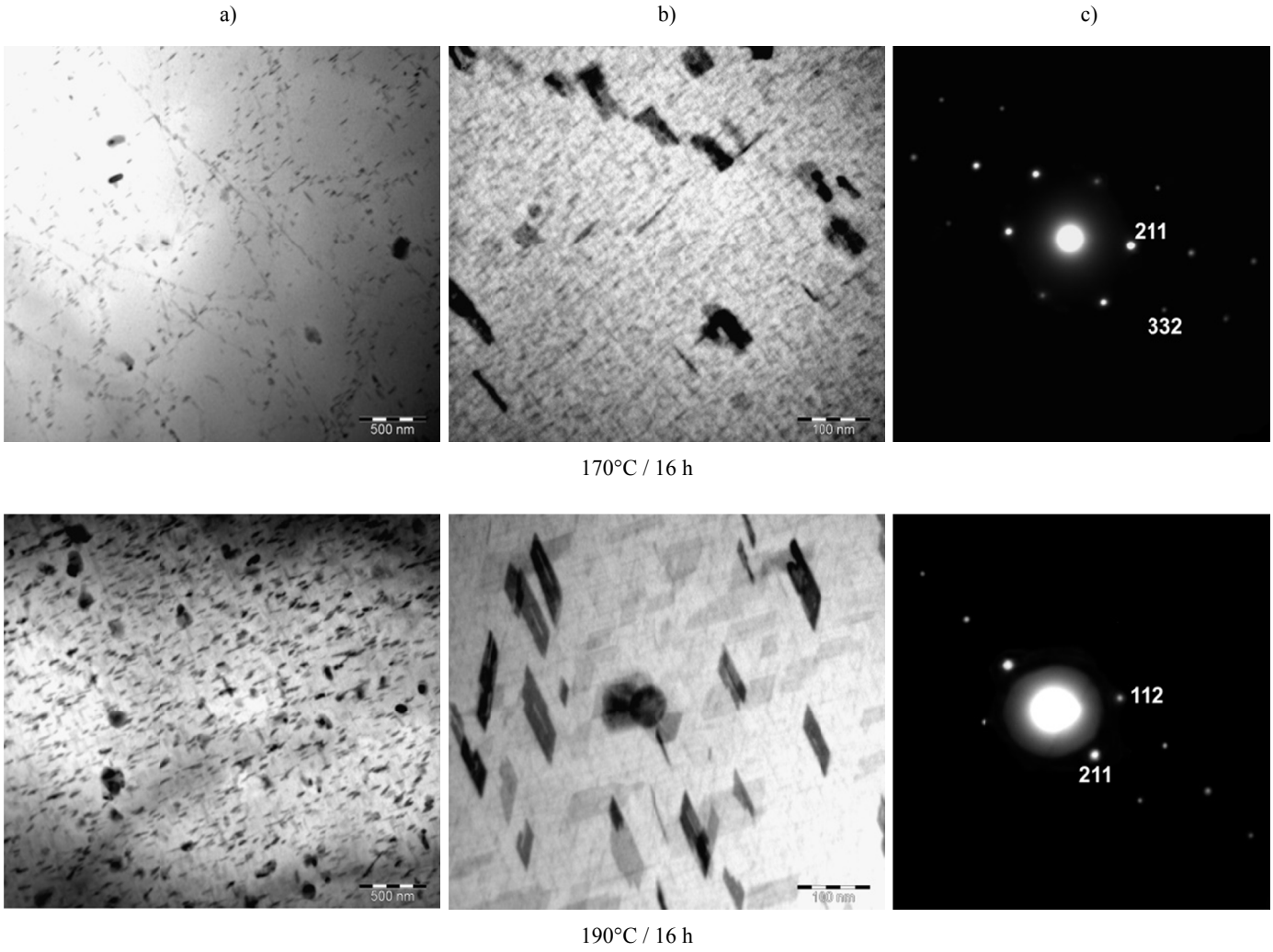

Fig. 4. TEM micrographs of the precipitation hardened AlSi9Cu3 specimens after precipitation hardening at two different temperatures of artificial aging; a) mag. 34 000×; b) 210 000×; c) SAED of Al_2Cu precipitates

TABLE 2

The average value of precipitates dimensions (width, length, thickness) and number per unit area (amount) of AlSi9Cu3 alloy

Artificial aging	Precipitates morphology							
	Oval particles			Platelets				Needles
	Width [nm]	Length [nm]	Amount [mm^{-2}]	Width [nm]	Thickness [nm]	Length [nm]	Amount [mm^{-2}]	Length [nm]
170°C / 16 h	70	140	9.10^5	30	2-4	60	5.10^7	15-20
190°C / 16 h	80	150	34.10^5	50	2-4	75	10.10^7	15-20

4. Conclusion

The present study describes effect of heat treatment (T4, T6 at 170°C and T6 at 190°C) on the properties of secondary AlSi9Cu3 cast alloy. The study confirms that structure changes (spheroidisation of Si particles, fragmentation and dissolution of intermetallic phases and ternary eutectic, and creating of dispersed intermetallic precipitates) depend on precipitation hardening of this experimental material and these changes led to increasing properties of this alloy (because the overall matrix was strengthened by a mechanism called the precipitation strengthening). The results of mechanical properties, SEM and TEM study show, that the „optimum'' schedule for mechanical properties is as follows: solution treatment: 4 h at 515°C; water quenching at 50°C; artificial aging: 16 h at 170°C.

Acknowledgements

This work has been supported by Scientific Grant Agency of Ministry of Education of Slovak republic N°1/0533/15, N°044ŽU-4/2014.

REFERENCES

[1] S.K. Das, Materials Science Forum **519-521**, 1239-1244 (2006).

[2] C.T. Rios, R. Caram, C. Bolfarini, W.J. Botta, C.S. Kiminami, Acta Microscopia **12**, 77-82 (2003).

[3] R. Li, AFS Transaction **26**, 777-783 (1996).

[4] C.F. Tan, M.R. Said, Chiang Mai Journal of Science **36** (3), 276-286 (2009).

[5] M. Uhríčik, P. Palček, A. Soviarová, P. Snopiński, Manufacturing Technology **14** (3), 470-467 (2014).

[6] M. Uhríčik, Z. Dresslerová, A. Soviarová, P. Palček, Production Engineering Archives **6** (1), 17-20 (2015).

[7] M.A. Moustafa, F.H. Samuel, W.H. Doty, Journal of Materials Science **38** (22), 1-12 (2003).

[8] S. Farahanya, A. Ourdjinia, M.H. Idrisi, S.G. Shabestarib, Thermochimica Acta **559**, 59-68 (2013).

[8] M. Timpel, N. Wanderka, R. Schlesiger, T. Yamamoto, N. Lazarev, N. Lazarev D. Isheim, G. Schmitz, S. Matsumura, J. Banhart, Acta Materialia **60** (9), 3920-3928 (2012).

[9] E.Tillová, M. Chalupová, L. Hurtalová, Evolution of Phases in a Recycled Al-Si Cast Alloy During Solution Treatment, in: Dr. Viacheslav Kazmiruk (Ed.), Scanning electron microscopy, Rijeka: InTech (2012).

[10] L. Kuchariková, E. Tillová, O. Bokůvka, Transport problems **11** (2), 117-122 (2016).

[11] J. Campbell, R.A. Harding, Solidification Defects in Castings. TALAT Lecture 3207, EAA – European Aluminium Association, 1994.

[12] K. Fukasawa, R. Mohri, T. Ohtake, T. Inoue, A. Kuroda, H. Kambe, M. Yoshida, Materials Transactions **57** (6), 959-965 (2016).

[13] S.C. Wang, M.J. Starink, International Materials Reviews **50**, 193-215 (2005).

[14] M. Vončina, J. Medved, P. Mrvar, Metalurgija **48** (1), 9-13 (2009).

[15] M. Vončina, A. Smolej, J. Medved, P. Mrvar, R. Barbič, RMZ--Materials and Geoenvironment **57** (3), 295-304 (2010).

[16] http://imechanica.org/files/handout4.pdf

[17] Y. Fan: Precipitation Strengthening of Aluminum by Transition Metal Aluminides. PhD Thesis, Worcester polytechnic institute, April 2012.

[18] S.P. Ringer, K. Hono, Materials Characterization **44**, 101-131 (2000).

[19] M. Abdulwahab, Australian Journal of Basic and Applied Sciences **2** (4), 839-843 (2008).

[20] R.R. Ambriz, D. Jaramillo, Mechanical behavior of precipitation hardened aluminium alloys welds. in: Dr. Viacheslav Kazmiruk (Ed.), Scanning electron microscopy, Rijeka: InTech (2014).

[21] N.A. Belov, D.G. Eskin, A.A. Aksenov, Multicomponent Phase Diagrams-Applications for Commercial Aluminum Alloys. Oxford : Elsevier (2005).

[22] http://www.limatherm.com/img/fck/8910041/limatherm/File/Technical%20information/Aluminium%20specification.pdf

[23] L. Hurtalová, E. Tillová, M. Chalupová, Key Engineering Materials **586**, 137-140 (2014).

[24] L. Hurtalová, E. Tillová, M. Chalupová, Key Engineering Materials **592-593**, 433-436 (2014).

[25] L. Hurtalová, E. Tillová, M. Chalupová, Engineering Transactions **61** (3), 197-218 (2013).

[26] Ch. Cáceres, Journal of Materials Enginneering Performance **9** (2), 215-221 (2000).